

THE TOTEM EXPERIMENT AT LHC

Giuseppe Latino

(for the TOTEM Collaboration)

Siena University & Pisa INFN, Physics Dept., Via Roma, 56 - 53100 Siena, Italy

e-mail: giuseppe.latino@pi.infn.it

Abstract

The TOTEM experiment at the CERN LHC is here presented. After an overview of the experimental apparatus, the measurement of the total pp cross section, elastic scattering and diffractive phenomena is described. This physics programme will allow to distinguish among different models of soft proton interactions.

1 Introduction

The TOTEM experiment ¹⁾ at the LHC is designed and optimized to measure the total pp cross section with a precision of about 1÷2%, to study the nuclear elastic pp cross section over a wide range of the squared four-momentum transfer $-t$ ¹ ($10^{-3} \text{ GeV}^2 < |t| < 10 \text{ GeV}^2$) and to perform a comprehensive physics programme on diffractive dissociation processes partially in cooperation with the CMS experiment. In order to fulfill its physics programme, complementary to the programme of the general-purpose experiments at the LHC, the TOTEM experiment has to cope the challenge of triggering and recording events in the very forward region with a good acceptance for particles produced at very small angles with respect to the beam. Based on the “luminosity independent” method the evaluation of the total cross section with such a small error will in particular require simultaneous measurement of the pp elastic scattering cross section $d\sigma/dt$ down to $|t| \sim 10^{-3} \text{ GeV}^2$ (to be extrapolated to $t = 0$) as well as of the pp inelastic interaction rate. In particular, the detection of elastically scattered protons at a location very close to the beam (indeed inside the beam-pipe itself) is required together with particle detection with the largest possible coverage in order to reduce losses on inelastic events detection to a few percent.

The TOTEM apparatus is located on both sides of the interaction point IP5, the same LHC experimental area as CMS ²⁾. The T1 and T2 tracking detectors are embedded inside the forward region of CMS (see fig.1, top). Charged track reconstruction in the pseudo-rapidity² range of $3.1 \leq |\eta| \leq 6.5$ is performed by these two inelastic telescopes and complemented at very high $|\eta|$ by detectors located in special movable beam-pipe insertion called “Roman Pots” (RP) which, being placed about 147 m and 220 m from IP5 (see fig.1, bottom), are designed to detect “leading” protons (scattered elastically or quasi-elastically from the interaction) at few mm from the beam center with a scattering angle down to few μrad .

The combination of the CMS and TOTEM experiments represents the largest acceptance detector ever built at a hadron collider which will also allow the study of a wide range of physics processes in diffractive interactions with an unprecedented coverage in rapidity. For this purpose the TOTEM data acquisition system (DAQ) is designed to be compatible with the CMS DAQ in order to make common data taking possible at a later stage.

In the following, after a brief description of the experimental apparatus, the main features of the TOTEM physics programme will be presented.

¹ In the relativistic limit and for small scattering angles: $|t| \sim (p\theta)^2$, where p is the proton momentum and θ is the scattering angle with respect to the original beam direction.

² Pseudo-rapidity is defined as $\eta = -\ln(\tan\frac{\theta}{2})$.

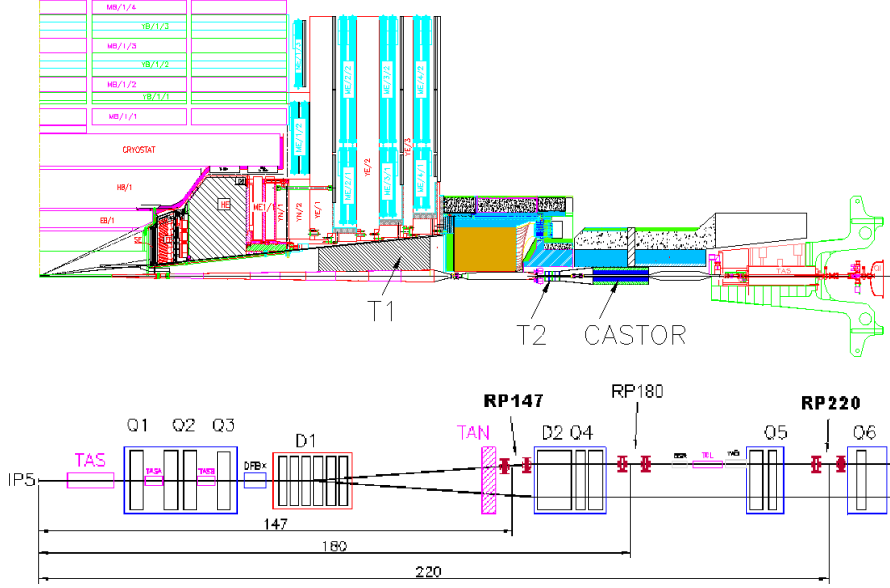


Figure 1: *Top: the TOTEM forward trackers T1 and T2 embedded into the forward region of the CMS detector. Bottom: TOTEM Roman Pots location along the LHC beam line at a distance about 147 m (RP147) and 220 m (RP220) from the interaction point IP5, RP180 being another possible location at the moment not equipped. All TOTEM detector components are located on both sides of IP5.*

2 Detector Overview

The TOTEM experimental setup comprises “Roman Pots” detectors to measure leading protons elastically scattered at very small angles within the beam pipe and the T1 and T2 inelastic telescopes providing charged track reconstruction for $3.1 < |\eta| < 6.5$ with a 2π coverage and with a very good efficiency in order to minimize losses (see fig.1). T1 and T2 track reconstruction will also allow trigger capability with acceptance greater than 95% for all inelastic events³ as well as the reconstruction of the event interaction vertex so that background events (mainly from beam-gas interactions and halo muons)³⁾ can be rejected. Furthermore, the T1 and T2 detectors will provide tracking in front of the CMS HF (T1) and Castor (T2) very forward calorimeters so that the

³ About 99.5% of all non-diffractive minimum bias events and about 84 % of all diffractive events have charged particles within the geometrical acceptance of T1 and T2 so that they are triggerable with these detectors.

combination of these detectors can allow, for instance, a more complete study of “rapidity gaps”⁴ and particle/energy flows in the very forward region.

The read-out of all TOTEM sub-detectors is based on the digital VFAT chip⁴) which is a tracking front-end ASIC specifically designed for the TOTEM experiment and characterized by trigger capabilities.

2.1 Roman Pots

The detection of very forward protons is performed by movable beam insertions, called “Roman Pots” (RP), hosting silicon detectors inside a secondary vacuum vessel (called “Pot”) which are moved very close to the beam into the primary vacuum of the machine through vacuum bellows. In this way the detectors can be put in a safe position when conditions of not stable beams are present (like at the very begin of a run), while are kept at the same time separated from the primary vacuum of the machine which is so preserved from an uncontrolled out-gassing of the detector materials. Two RP stations are installed on both sides from the interaction point IP5 on the beam pipe of the outgoing beam at a distance of about 147 m and at 220 m, a position chosen according to the constraints given by the space available among the LHC machine components and by the special optics used by TOTEM. A magnetic dipole between the two RP stations provides a magnetic spectrometer allowing an accurate proton momentum reconstruction. Each RP station is composed of two units (see fig.2, left) in order to have a lever arm for local track reconstruction and trigger selections by track angle. Each unit consists of 3 pots, 2 approaching the beam vertically from the top and the bottom and one horizontally which completes the acceptance for diffractively scattered protons (see fig.2, right). The overlap of the detectors in the horizontal pots with the ones in the vertical pots allows a correlation of their positions via common particle tracks. This is used for the alignment of the three pots in an unit, the absolute alignment with respect to the beam being given by Beam Position Monitors (BPM) located in the vacuum chamber of the vertical pots.

Each pot contains a stack of 10 planes of novel silicon strip “edgeless” detectors, half of which have their strips oriented at an angle of $+45^\circ$ and half at an angle of -45° with respect to the edge facing the beam. Each plane has 512 strips with a pitch of $66 \mu\text{m}$ allowing a single hit resolution of about $20 \mu\text{m}$. In order to detect protons elastically scattered at angles down to few μrad at the RPs locations, these detectors need to have their active area edge moved as close to the beam as $\sim 1 \text{ mm}$. Consequently, their edge dead area had to be

⁴ A rapidity gap, a region of pseudo-rapidity devoid of particles, is a typical signature for diffractive processes which are characterized by a hadronic color singlet exchange with vacuum quantum numbers, for which the Pomeron is one model.

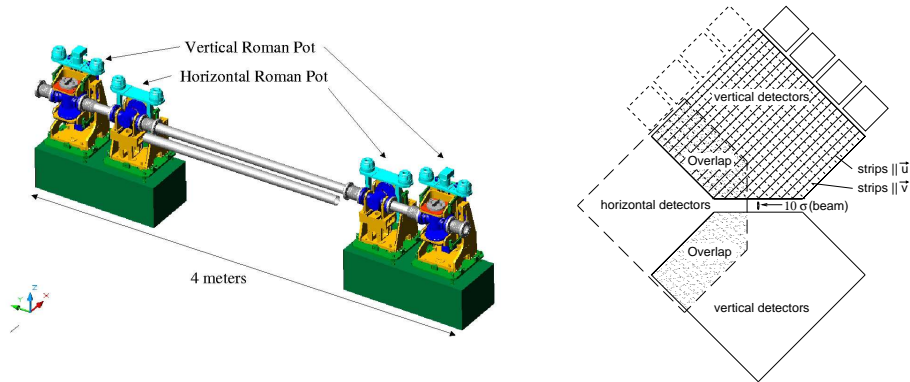


Figure 2: *Left: one TOTEM Roman Pot station. Right: arrangement of silicon detectors inside two vertical and one horizontal pots at a RP unit.*

greatly minimized so that a new “edgeless planar silicon” detector technology has been developed for TOTEM RPs where a current terminating structure allows to reduce to only $50\ \mu\text{m}$ the insensitive decoupling area detector edge and sensitive volume ⁵⁾. For the same reason the stainless steel bottom foil of the pot (the one facing the beam) has been reduced to a thickness of $150\ \mu\text{m}$, while the pot window in front of the detector active area is $500\ \mu\text{m}$ thick.

Irradiation studies on these silicon detectors, performed at the TRIGA reactor in Ljubljana at different neutron fluxes up to $10^{14}\ \text{1 MeV n/cm}^2$ and with $24\ \text{GeV}$ protons at CERN with a radiation up to $1.4 \times 10^{14}\ \text{p/cm}^2$, have shown similar aging effects as for devices using standard voltage terminating structures. Calculations of the diffractive proton flux hitting the detectors indicate that the present detectors will probably be working up to an integrated luminosity of about $1\ \text{fb}^{-1}$. To cope with higher luminosities, TOTEM has initiated an INTAS project to develop radiation harder edgeless detectors ⁶⁾.

2.2 T1 and T2 tracking detectors

The T1 telescope covers the pseudo-rapidity range $3.1 < |\eta| < 4.7$ on both sides of IP5. Each telescope arm consists of five planes, equally spaced in z , formed by six trapezoidal “Cathode Strip Chambers” (CSC) ¹⁾ (see fig.3, left). The detector sextants in each plane are rotated with respect to each other by angles varying from -6° to $+6^\circ$ in steps of 3° in order to improve the pattern recognition for track reconstruction and to reduce the localized concentration of material in front of the CMS HF calorimeter. The TOTEM CSCs have a detector design similar to CMS CSC muon chambers with a gas gap of 10

mm and a gas mixture of Ar/CO₂/CF₄ (40%/50%/10%). In these detectors the segmentation of cathode planes into parallel strips gives, combining their read-out with the one from anode wires, three measurements of the coordinates of the particle traversing the detector plane. Anode wires (with a pitch of 3 mm) give radial coordinate measurement which is also used for level-1 trigger information, while cathode strips (with a pitch of 5 mm) are rotated by $\pm 60^\circ$ with respect to the wires. Beam tests on final prototypes have shown a spatial resolution of about 0.8 mm when using VFAT digital read-out. Aging studies performed at the CERN Gamma Irradiation Facility have shown no loss of performance after an irradiation resulting in a total charge integrated on the anode wires of 0.065 C/cm, which corresponds to an accumulated dose equivalent to about 5 years of running at luminosities of $10^{30}\text{cm}^{-2}\text{s}^{-1}$.

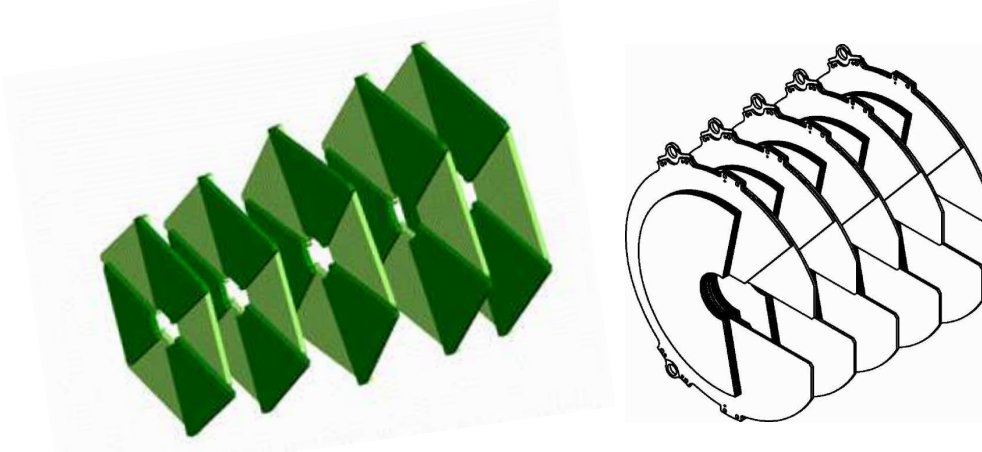


Figure 3: *Left: one arm of the TOTEM T1 telescope. Right: one half-arm of the TOTEM T2 telescope.*

The T2 telescope, based on novel “Gas Electron Multiplier” (GEM) technology ⁷⁾, extends charged track reconstruction to the rapidity range $5.3 < |\eta| < 6.5$ ¹⁾. Placed 13.5 m away from both sides of IP5, each T2 arm consists of a set of 20 triple-GEM detectors having an almost semicircular shape with an inner radius matching the beam pipe. Ten aligned detectors planes, mounted “back-to-back”, are combined to form one T2 semi-arm on each side of the vacuum pipe (see fig.3, right). To avoid efficiency losses, the angular coverage of each detector is more than 180° . GEMs are gas-filled detectors, already successfully adopted in other experiments such as COMPASS and LHCb, which have been considered for the design of the TOTEM very forward T2 telescopes thanks to their characteristics, in particular: good spatial resolution, excellent rate capability and good resistance to radiation. Furthermore, GEM detectors

are also characterized by the advantageous decoupling of the charge amplification structure from the charge collection and read-out structure which allows an easy implementation of the design for a given apparatus. The T2 GEMs⁸⁾ use the same baseline design as the ones adopted in COMPASS with a triple-GEM structure, realized by separating three GEM foils by thin (2 mm) insulator spacers, adopted in order to reduce sparking probabilities while reaching typical total gas gains of about 8×10^3 with a relatively low voltage (around 500 V) applied to each GEM foil. The gas mixture is Ar/CO₂ (70%/30%). The read-out board, explicitly designed for TOTEM, has two separate layers with different patterns: one with 256x2 concentric circular strips, 80 μm wide and with a pitch of 400 μm , allowing track radial reconstruction, and the other with a matrix of 24x65 pads varying in size from 2x2 mm² to 7x7 mm² (for a constant $\Delta\eta \times \Delta\phi \sim 0.06 \times 0.017\pi$) providing level-1 trigger information as well as track azimuthal reconstruction. Final production detectors have been successfully tested in the 2007 beam test showing a spatial resolution in radial coordinate of about 100 μm with digital VFAT read-out. COMPASS triple-GEM detectors aging tests have shown that a charge up to 20 mC/mm² can be integrated on the read-out board without aging effects. This corresponds to run TOTEM for at least 1 year at luminosities of $10^{33}\text{cm}^{-2}\text{s}^{-1}$. It is so assumed that TOTEM T2 triple-GEM can be operated during the first 3 years of LHC running.

3 Physics Programme

Given its unique coverage for charged particles at high rapidities, TOTEM is an ideal detector for studying forward phenomena, including elastic and diffractive scattering. Its main physics goals, precise measurements of the total pp cross section σ_{tot} and of the elastic scattering over a large range in t , are of primary importance in order to distinguish among different models of soft proton interactions. Furthermore, as energy flow and particle multiplicity of inelastic events peak in the forward region, the large rapidity coverage and the proton detection on both sides of the interaction point allow the study of a wide range of physics processes in inelastic and diffractive interactions.

3.1 Total pp cross section

Fig. 4 summarizes the existing measurements of σ_{tot} from low energies up to collider and cosmic ray energies, also showing recent predictions for the energy dependence of σ_{tot} by fitting all available pp and $p\bar{p}$ scattering data according to different models⁹⁾. The dark error band shows the statistical errors to the best fit ($\sigma_{tot} = 111.5 \pm 1.2_{-2.1}^{+4.1}$ mb for the LHC energy), the closest dashed curves near it give the sum of statistical and systematic errors to the best fit

due to the discrepancy of the two Tevatron measurements, and the highest and lowest dotted curves show the total error bands (ranging in the 90÷130 mb interval) from all models considered. This large theoretical uncertainty is due to the current lack of a fully satisfactory theoretical explanation of the cross section in low momentum transfer collisions, their description relying on phenomenological models to be tuned on existing data. The large uncertainties of the cosmic ray data and the 2.6 standard deviations discrepancy between the two final results from the Tevatron give an extrapolation to the LHC energy ($\sqrt{s} = 14$ TeV) which is characterized by a wide range for the expected value of σ_{tot} , typically from 90 to 130 mb, depending on the model used for the extrapolation. More recent studies by other authors give predictions substantially within this range, with the exception of models with an explicit “hard” pomeron which give predictions at higher values¹⁰). TOTEM aims to measure σ_{tot} with a precision down to $\sim 1\%$ (or ~ 1 mb), therefore allowing to discriminate among the different models.

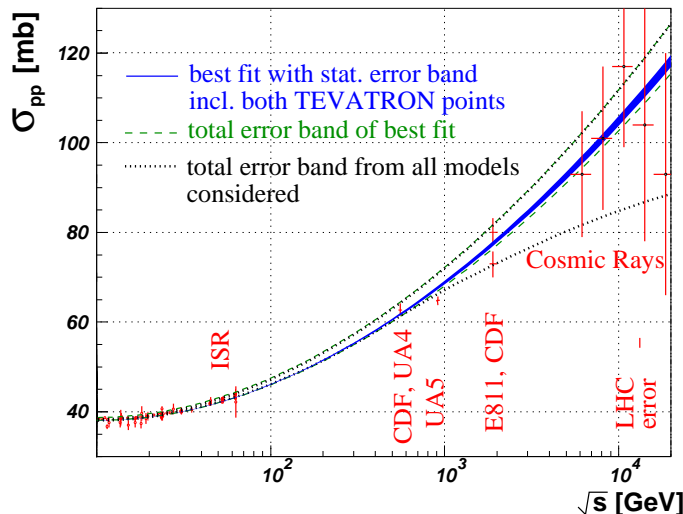


Figure 4: Fits from the COMPETE collaboration to all available pp and $p\bar{p}$ scattering data⁹).

In absence of an accurate determination of the LHC luminosity the measurement of σ_{tot} will be based on the “luminosity independent” method which combines the optical theorem, relating σ_{tot} to the imaginary part of the forward scattering amplitude and leading to the following equation:

$$\mathcal{L}\sigma_{tot}^2 = \frac{16\pi}{1 + \rho^2} \cdot \left. \frac{dN_{el}}{dt} \right|_{t=0} \quad (1)$$

with the total rate equation:

$$\mathcal{L} \sigma_{tot} = N_{el} + N_{inel} \quad (2)$$

resulting in a system of 2 equations which can be solved for σ_{tot} and \mathcal{L} , which are so expressed as a function of measurable rates:

$$\sigma_{tot} = \frac{16\pi}{1 + \rho^2} \cdot \frac{dN_{el}/dt|_{t=0}}{N_{el} + N_{inel}} \quad (3)$$

$$\mathcal{L} = \frac{1 + \rho^2}{16\pi} \cdot \frac{(N_{el} + N_{inel})^2}{dN_{el}/dt|_{t=0}} \quad (4)$$

TOTEM will then measure σ_{tot} and the luminosity \mathcal{L} independently by experimentally measuring: the inelastic rate N_{inel} consisting of non-diffractive minimum bias events (~ 65 mb at LHC) and diffractive events (~ 18 mb at LHC) which will be measured by T1 and T2; the total nuclear elastic rate N_{el} (~ 30 mb at LHC) and the nuclear part of the elastic cross section extrapolated to $t = 0$ (optical point) $dN_{el}/dt|_{t=0}$, measured by the Roman Pot system. For the rate measurements it is important that all TOTEM detector systems have trigger capability. The expected uncertainty of the extrapolation to $t = 0$ depends on the acceptance for elastically scattered protons at small t -values, hence on the beam optics. The ρ parameter, defined by:

$$\rho = \frac{\mathcal{R}[f_{el}(0)]}{\mathcal{I}[f_{el}(0)]} \quad (5)$$

where $f_{el}(0)$ is the forward nuclear elastic scattering amplitude, has to be taken from external theoretical predictions, e.g. ⁹). Since $\rho \sim 0.14$ enters only in a $1 + \rho^2$ term, its impact is small.

A precise measurement of small scattering angles for the protons requires the beam angular divergence to be as small as possible, hence special runs with high machine optics β^* are required. The consequent increase in beam size at the interaction point and the zero crossing angle technically related to this optics configuration also require a small number of bunches, in order to avoid extra interactions between the colliding beams inside the common vacuum chamber. Consequently the typical instantaneous luminosity for the TOTEM σ_{tot} measurement at level of $\sim 1\%$, obtained with an approved optics characterized by $\beta^* = 1540$ m and 43 bunches, will be of the order of 10^{28} $\text{cm}^{-2}\text{s}^{-1}$. The requirement of a special injection optics for the optimal $\beta^* = 1540$ m configuration makes it probably not available at the early beginning of LHC. Another approved special beam optics with $\beta^* = 90$ m (and a luminosity close to 10^{30} $\text{cm}^{-2}\text{s}^{-1}$), achievable without modifying the standard LHC injection optics, will allow a preliminary σ_{tot} measurement at the level of about

5% uncertainty as well as an excellent measurement of the momentum loss of diffractive protons, opening the studies of soft and semi-hard diffraction, the latter in combination with the CMS detectors. After having understood the initial measurements and with improved beams at $\beta^* = 1540$ m, a precision around 1% should be achievable, provided an improved knowledge of the optical functions⁵ and an alignment precision of the RP station better than 50 μ m are obtained.

Given the high value of measured rates, the statistical error on σ_{tot} measurement will be substantially negligible after few hours of data taking even at low luminosity runs. The vertex reconstruction will allow to largely reject the background from beam-gas (dominant) and beam halo events to a negligible rate. The systematic error for the measurement with $\beta^* = 90$ m will be dominated by the extrapolation of nuclear elastic cross section to $t = 0$ ($\sim 4\%$ for $|t|$ measured down to about $|t| = 10^{-2}$ GeV²), while for the $\beta^* = 1540$ m measurement the total inelastic rate will give the main systematic uncertainty which will be dominated by trigger losses in Single Diffraction events ($\sim 0.8\%$)⁶. The theoretical uncertainty related to the estimate of the ρ parameter is expected to give a relative uncertainty contribution of less than 1.2% (considering for instance the full error band on ρ extrapolation as derived in ref ⁹). Combining all relevant uncertainties by error propagation for the equations 3 and 4, also taking into account the correlations, gives a relative error of about 5% (7%) for the measurement of $\sigma_{tot}(\mathcal{L})$ with $\beta^* = 90$ m and of about 1÷2% (2%) for $\sigma_{tot}(\mathcal{L})$ with $\beta^* = 1540$ m ⁶.

⁵ The optical functions determine the explicit path of the particle through the magnetic elements and depend mainly on the position along the beam line (i.e. on all the magnetic elements traversed before reaching that position and their setting which is optics dependent) but also on the particle parameters at the IP.

⁶ Dedicated studies have shown that Single and Double Diffraction events are responsible for the major loss in the inelastic rate. With a single-arm trigger (in coincidence with a leading proton in the opposite side RP for the single diffractive events) a fraction of these events, corresponding to ~ 2.8 mb, escapes detection. The lost events are mainly those with a very low mass (below ~ 10 GeV/ c^2), since all their particles are produced at pseudo-rapidities beyond the T2 tracker acceptance. The fraction of these lost events can be estimated by extrapolation to low masses so to allow the determination of the total inelastic rate. For Single Diffraction, the extrapolated number of events differs from the simulation expectations by 4%, corresponding to a 0.6 mb uncertainty on the total cross-section. The same estimate for Double Diffraction and Double Pomeron Exchange gives a 0.1 mb and 0.2 mb uncertainty, respectively.

3.2 Nuclear elastic pp scattering

Most of the interest in large impact parameter collisions is related to nuclear (hadronic) elastic scattering and to soft inelastic diffraction, both characterized, e.g., by the exchange of hadronic colour singlets. Fig. 5 shows the differential cross section of elastic pp interactions at $\sqrt{s} = 14 \text{ TeV}$ ¹¹⁾ as predicted by different models ¹²⁾. Several regions with different behavior can be distinguished

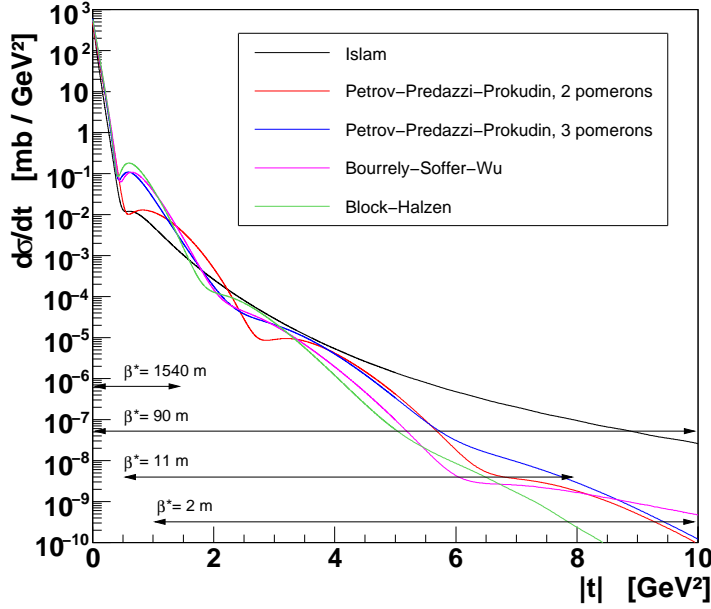


Figure 5: *Differential cross section of elastic scattering at $\sqrt{s} = 14 \text{ TeV}$ as predicted by different models ¹²⁾. The t -acceptance ranges for different optics settings are also shown.*

when different t -ranges are considered at increasing $|t|$ (which means looking deeper into the proton at smaller distance). The Coulomb region, where elastic scattering is dominated by one photon exchange ($d\sigma/dt \sim 1/t^2$), is characterized by $|t| \leq 10^{-5} \text{ GeV}^2$. In the intermediate region for $|t|$ up to 0.002 GeV^2 , the hadronic and Coulomb scattering interfere, complicating the extrapolation of the nuclear cross section to $t = 0$. The hadronic region, described in a simplified way, e.g., by “single-Pomeron exchange” with an approximately exponential cross section ($d\sigma/dt \sim e^{-B|t|}$) at its lower border, is expected for $0.002 < |t| < 0.4 \text{ GeV}^2$.

The predictions of different models shown in Fig. 5 have been obtained

by fitting the differential cross section data at lower measured energies starting at the ISR energies. The shown results are based on the eikonal model. The influence of the Coulomb scattering at lower $|t|$ values has been described with the help of West and Yennie type of the total elastic scattering amplitude¹¹⁾. It is still an open question if a different approach could be used in order to remove the discrepancy on the elastic impact parameters introduced by the West and Yennie approach^{11, 13)}.

It is evident that the interference region and the beginning of hadronic region are important for the extrapolation of hadronic dN_{el}/dt to $t = 0$, needed for determination of σ_{tot} . The t -dependence of $B(t) = \frac{d}{dt} \ln \frac{d\sigma}{dt}$, shows slight model dependent deviations¹¹⁾ from exponential shape, giving a theoretical uncertainty contribution to the systematic error of the total cross section measurement. The fit is typically performed with a quadratic polynomial parametrization in the $|t|_{min} < |t| < 0.25 \text{ GeV}^2$ interval, where $|t|_{min}$ depends on the acceptance for protons elastically scattered at small angles, which is related to the beam angular divergence. The expected uncertainty on the extrapolation to $t = 0$ will be related to $|t|_{min}$ ($|t|_{min} \sim 0.002 (0.04) \text{ GeV}^2$ for $\beta^* = 1540 (90) \text{ m}$), hence it will depend on the beam optics. The diffractive structure of the proton is then expected in the $|t| > 0.4 \text{ GeV}^2$ region. Finally, for $|t| \geq 1.5 \div 3 \text{ GeV}^2$ there is the domain of central elastic collisions at high $|t|$ which might be described by perturbative QCD, e.g., in terms of three gluon exchange with a predicted cross section proportional to $|t|^{-8}$ ¹⁴⁾.

We can see from fig. 5 that there is a model dependence of the predictions which is very pronounced at high $|t|$. To discriminate among different models it is thus important to precisely measure the elastic scattering over the largest possible t -region. As shown in fig. 5 TOTEM can study different t -ranges depending on the LHC optics setting. Under different beam optics and running conditions TOTEM will cover the $|t|$ -range from $2 \times 10^{-3} \text{ GeV}^2$ to about 10 GeV^2 spanning the elastic cross section measurement for over 11 orders of magnitude.

3.3 Diffraction and inelastic processes

Fig. 6 shows the typical event topology for non diffractive (Minimum Bias) and diffractive processes together with the associated cross sections, as expected at the LHC. Diffractive scattering processes (Single Diffraction, Double Diffraction, “Double Pomeron Exchange”, and higher order “Multi Pomeron” processes) together with the elastic scattering one, represent about 50% of the total cross section. Nevertheless, many details of these processes with close ties to proton structure and low-energy QCD are still poorly understood. The majority of diffractive events exhibits intact (“leading”) protons in the final state, characterized by their t and by their fractional momentum loss $\xi \equiv \Delta p/p$,

most of which (depending on the beam optics) can be detected in the RP detectors. Already at an early stage, TOTEM will be able to measure ξ -, t - and mass-distributions in soft Double Pomeron and Single Diffractive events. The integration of TOTEM with the CMS detector will offer the possibility of more detailed studies of the full structure of diffractive events, with the optimal reconstruction of one or more sizeable rapidity gaps in the particle distributions which can be obtained when the detectors of CMS and TOTEM will be combined for common data taking with an unprecedented rapidity coverage, as detailed in ref ³). For this purpose the TOTEM triggers, combining information from the inelastic detectors and the silicon detectors in the RPs, are designed to be also incorporated into the general CMS trigger scheme.

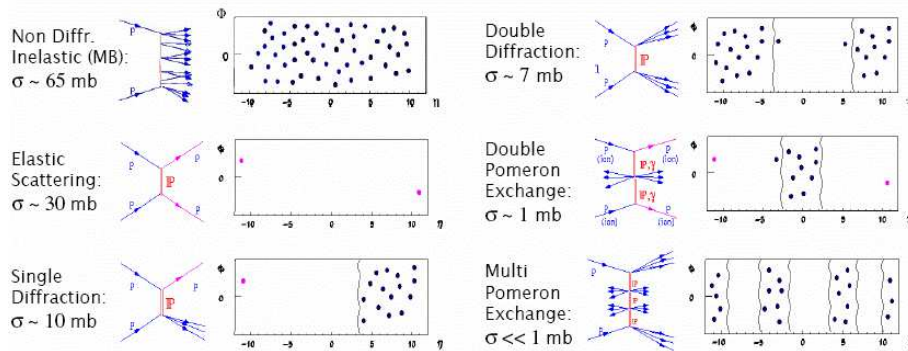


Figure 6: *Typical event topology for non diffractive (Minimum Bias) and diffractive processes in the pseudorapidity-azimuth plane. The associated cross sections, as estimated for the LHC, are also reported.*

TOTEM will also provide a significant contribution to the understanding of very high energy cosmic ray physics as it will give accurate informations on the basic properties of pp collisions at the maximum accelerator energy. A challenging issue in astrophysics is in fact represented by primary cosmic rays in the PeV (10^{15} eV) energy range and above. The LHC center of mass energy corresponds to a 100 PeV energy for a fixed target collision in the air. At the same time the LHC will provide a very high event rate relative to the very low rate of cosmic ray particles in this energy domain. Several high energy hadronic interaction models are nowadays available describing the nuclear interaction of primary cosmic ray entering the upper atmosphere and generating air showers. They predict energy flow, multiplicity and other quantities of such showers which characteristics are related to the nature of the primary interaction and to the energy and composition of the incident particle. There are large differences among the predictions of currently available models, with significant inconsis-

tencies in the forward region. Several quantities can be measured by TOTEM and CMS and compared with model predictions, among which: energy flow, elastic/total cross section, fraction of diffractive events, particle multiplicity. The study of the features of diffractive and inelastic events as measured in TOTEM and CMS may thus be used to validate/tune these generators³⁾.

4 Summary and Conclusions

The TOTEM experiment will be ready for data taking since the very beginning of the LHC start. Running under all beam conditions, it will be able to perform an important and exciting physics programme involving total and nuclear elastic scattering pp cross section measurements as well as diffractive processes studies. Special high β^* runs will be needed in order to perform an optimal measurement of total pp cross section at the level of $\sim 1 \div 2$ % (for $\beta^* = 1540$ m). An early measurement is foreseen with $\beta^* = 90$ m (more easily achievable) with a relative error at the level of ~ 5 %. The measurement of elastic scattering in the range $10^{-3} \text{ GeV}^2 < |t| < 10 \text{ GeV}^2$ will allow to distinguish among a wide range of predictions according to current theoretical models. Finally, a common physics programme with CMS on soft and hard diffraction as well as on forward particle production studies will also be pursued.

5 Acknowledgements

I'm very grateful to the Conference Organizers, Giorgio Bellettini, Giorgio Chiarelli and Mario Greco for their kind invitation and warm hospitality at this very profitable and pleasant annual appointment for the HEP Community in La Thuile. I would like also to thank my Colleagues of the TOTEM Collaboration for their hard work in the development of the experiment and for precious input to this presentation.

References

1. TOTEM Technical Design Report, CERN-LHCC-2004-002; addendum CERN-LHCC-2004-020 (2004).
2. CMS Physics Technical Design Report, Volume I: Detector performance and software, CERN-LHCC-2006-001 (2006);
3. The CMS and TOTEM diffractive and forward physics working group, Prospects for Diffractive and Forward Physics at the LHC, CERN-LHCC-2006-039/G-124 (2006).

4. P. Aspell *et al.*, VFAT2 : A front-end system on chip providing fast trigger information, digitized data storage and formatting for the charge sensitive readout of multi-channel silicon and gas particle detectors,
Published in *Prague 2007, Electronics for particle physics* 63 (2007).
5. E. Noschis *et al.*, Final size planar edgeless silicon detectors for the TOTEM experiment, Nucl. Instr. & Meth. **A563**, 41 (2006).
6. G. Anelli *et al.* (TOTEM Collaboration), The TOTEM Experiment at the LHC, *in preparation*.
7. F. Sauli, GEM: A new concept for electron amplification in gas detectors, Nucl. Instr. & Meth. **A386**, 531 (1997).
8. S. Lami *et al.*, A triple-GEM telescope for the TOTEM experiment, Nucl. Phys. **B172**, 231 (2007).
9. J.R. Cudell *et al.* (COMPETE Collaboration), Benchmarks for the Forward Observables at RHIC, the Tevatron-Run II, and the LHC, Phys. Rev. Lett. **89**, 201801 (2002).
10. M.G. Ryskin *et al.*, Soft diffraction at the LHC: a partonic interpretation, Eur.Phys.J. **C54**, 199 (2008).
A. Achilli *et al.*, Total cross-section and rapidity gap survival probability at the LHC through an eikonal with soft gluon resummation, Phys.Lett. **B659**, 137 (2008).
11. V. Kandrát *et al.*, To the theory of high-energy elastic nucleon collisions, in Forward Physics and QCD, Proceedings of the 12th International Conference on Elastic and Diffractive Scattering, DESY - Hamburg May 2007, DESY-PROC-2007-02, p.273 (2007).
12. M. M. Islam *et al.*, Near forward pp elastic scattering at LHC and nucleon structure, Int. J. Mod. Phys. **A21**, 1 (2006).
C. Bourrely *et al.*, Impact-picture phenomenology for $\pi^\pm p$, $K^\pm p$ and pp , $\bar{p}p$ elastic scattering at high energies, Eur. Phys. J. **C28**, 97 (2003).
V. A. Petrov *et al.*, Coulomb interference in high-energy pp and $\bar{p}p$ scattering, Eur. Phys. J. **C28**, 525 (2003).
M. M. Block *et al.*, Photon-proton and photon-photon scattering from nucleon-nucleon forward amplitudes, Phys. Rev. **D60**, 054024 (1999).
13. V. Kandrát *et al.*, Limited validity of West and Yennie interference formula for elastic scattering of hadrons, Phys. Lett. B **656**, 182 (2007).
14. A. Donnachie, P. V. Landshoff, Elastic scattering at large t , Z. Phys. **C2**, 55 (1979), Erratum-ibid. **C2**, 372 (1979);
The interest of large $-t$ elastic scattering, Phys. Lett. **B387**, 637 (1966).